JVI Journals.ASM.org

Myd88-Dependent Toll-Like Receptor 7 Signaling Mediates Protection from Severe Ross River Virus-Induced Disease in Mice

Lauren M. Neighbours,[b,c] Kristin Long,[a,c] Alan C. Whitmore,[a,c] and Mark T. Heise[a,b,c]

Department of Genetics, University of North Carolina at Chapel Hill, Chapel Hill, North Carolina, USA[a]; Department of Microbiology and Immunology, University of North Carolina at Chapel Hill, Chapel Hill, North Carolina, USA[b]; and Carolina Vaccine Institute, University of North Carolina at Chapel Hill, Chapel Hill, North Carolina, USA[c]

Arthralgia-associated alphaviruses, including chikungunya virus (CHIKV) and Ross River virus (RRV), pose significant public health threats because of their ability to cause explosive outbreaks of debilitating arthralgia and myalgia in human populations. Although the host inflammatory response is known to contribute to the pathogenesis of alphavirus-induced arthritis and myositis, the role that Toll-like receptors (TLRs), which are major regulators of host antiviral and inflammatory responses, play in the pathogenesis of alphavirus-induced arthritis and myositis has not been extensively studied. Using a mouse model of RRV-induced myositis/arthritis, we found that myeloid differentiation primary response gene 88 (Myd88)-dependent TLR7 signaling is involved in protection from severe RRV-associated disease. Infections of Myd88- and TLR7-deficient mouse strains with RRV revealed that both Myd88 and TLR7 significantly contributed to protection from RRV-induced mortality, and both mouse strains exhibited more severe tissue damage than wild-type (WT) mice following RRV infection. While viral loads were unchanged in either Myd88 or TLR7 knockout mice compared to WT mice at early times postinfection, both Myd88 and TLR7 knockout mice exhibited higher viral loads than WT mice at late times postinfection. Furthermore, while high levels of RRV-specific antibody were produced in TLR7-deficient mice, this antibody had very little neutralizing activity and had lower affinity than WT antibody. Additionally, TLR7- and Myd88-deficient mice showed defects in germinal center activity, suggesting that TLR7-dependent signaling is critical for the development of protective antibody responses against RRV.

Mosquito-transmitted alphaviruses cause a variety of disease states in animals and humans, ranging from joint and muscle pain to severe neuropathology and encephalitis (17, 50, 65). Because of the wide distribution of their viral vectors and their ability to cause explosive outbreaks of debilitating arthralgia and myalgia, arthralgia-associated viruses such as chikungunya virus (CHIKV) and Ross River virus (RRV) are considered to be significant emerging disease threats (19, 23, 28, 51). Though rarely fatal, alphavirus-induced arthritis can be quite debilitating and can progress to chronic disease in a significant subset of individuals, thereby significantly affecting the patients' quality of life and placing substantial burdens on health care systems (20).

Several studies have demonstrated that immune pathology contributes to alphavirus-induced arthritis and myositis (21, 29–31, 37, 38). Mouse models of arthritogenic alphavirus infection have implicated inflammatory macrophages and complement in the development of alphavirus-induced disease (21, 29–31, 38, 39). However, the signaling pathways underlying alphavirus pathogenesis remain poorly understood, and further characterization of the pathways contributing to alphavirus-induced arthritis and myositis may lead to the development of more effective antiviral therapies to treat affected individuals (19).

Toll-like receptors (TLRs) are pattern recognition receptors that recognize conserved microbial patterns on pathogens, including bacteria, fungi, and viruses (26). Following TLR engagement and stimulation by invading microbes, specific adaptor molecules interact with the activated TLRs and then initiate downstream signaling cascades to promote innate immune responses and target the associated infection (62). Although TLRs have been found to play a role in many virally induced diseases, usually functioning in a protective capacity, and certain TLRs (including TLR1, -2, -3, -7, -8, and -9) and the TLR adaptor molecule myeloid differentiation primary response gene 88 protein (Myd88), have been found to be upregulated during alphavirus infection (35, 36, 57), the importance of TLRs in the pathogenesis of alphavirus-induced arthritis/myositis has not been elucidated.

To determine whether TLRs influence alphavirus pathogenesis, we evaluated the role of Myd88 in a mouse model of RRV-induced arthritis/myositis. Because Myd88 is essential for signaling by all TLRs except for TLR3 and partial TLR4 signaling, we chose first to focus our studies on Myd88 to determine whether RRV-induced disease is impacted by the absence of this central TLR signaling molecule (42, 55, 60, 62). Here we report that mice deficient in Myd88 developed more severe disease and RRV-induced mortality than RRV-infected wild-type (WT) C57BL/6J mice and that TLR7-deficient animals exhibited a phenotype almost identical to that of the Myd88-deficient mice during RRV infection. Moreover, mice deficient in TLR7 produced lower levels of neutralizing antibodies following RRV infection than WT animals, suggesting that Myd88-dependent TLR7 signaling is required for the control of RRV replication and for protection from severe RRV-induced disease.

MATERIALS AND METHODS

Virus stocks and cells. Viral stocks of the mouse-virulent T48 strain of Ross River virus (RRV) were generated from the full-length T48 cDNA clone (generously provided by Richard Kuhn, Purdue University) as previously described (27). Viral titers were determined by plaque assay on Vero cells as described below. Fresh and confluent Vero cell monolayers,

Received 7 March 2012 Accepted 16 July 2012
Published ahead of print 1 August 2012
Address correspondence to Mark T. Heise, heisem@med.unc.edu.

doi:10.1128/JVI.00601-12

grown in Dulbecco modified Eagle medium (DMEM)-F12 (Gibco) with 10% HyClone fetal bovine serum (FBS), 1% nonessential amino acids, 1% penicillin-streptomycin, 2.5% $NaHCO_3$ (Gibco), and 1% L-glutamine, were used for all plaque assay and Plaque reduction neutralization test (PRNT) assay experiments.

Mouse experiments. C57BL/6J wild-type (WT), TLR7-deficient ($TLR7^{-/-}$), and Myd88-deficient ($Myd88^{-/-}$) mice were obtained from The Jackson Laboratory (Bar Harbor, ME) and bred in house. $TLR7^{-/-}$ and $Myd88^{-/-}$ mice were both maintained on a C57BL/6 background. Animal husbandry and experiments were performed in accordance with all University of North Carolina, Chapel Hill, Institutional Animal Care and Use Committee guidelines. All mouse studies were performed in a biosafety level 3 laboratory. Twenty-four-day-old mice were used for all *in vivo* studies. Mice were anesthetized with isoflurane (Halocarbon Laboratories) prior to subcutaneous inoculation in the left rear footpad with 10^3 PFU of virus in phosphate-buffered saline (PBS) diluent in a 10-μl volume. Mock-infected animals were inoculated with PBS diluent alone. Mice were weighed and monitored daily for clinical disease signs. Disease scores were determined by assessing grip strength, hind limb weakness, and altered gait as described previously (39). Briefly, mice were scored on a scale from 0 to 6, where 0 indicated no disease signs, 1 or 2 indicated ruffled fur and mild hind limb weakness, 3 or 4 indicated moderate hind limb weakness and altered gait, 5 indicated severe hind limb weakness and dragging of hind limbs, and 6 indicated that the mice were immobile (moribund) and unable to consume adequate amounts of food and water, thus meeting euthanasia criteria.

Viral titers. To determine viral titers in RRV-infected murine tissues, mice were anesthetized and sacrificed by exsanguination. Quadriceps tissues were excised and homogenized, and serum was extracted prior to freezing at −80°C until viral titers were assessed. Viral tissues were thawed on ice and subsequently diluted in PBS diluent in 10-fold dilutions. After dilution, 200 μl of infected tissue samples were pipetted into each well of 70% confluent Vero cells in duplicate for each dilution. The samples were incubated on the cells for 1 h at 37°C in a CO_2 incubator and gently agitated every 15 min to ensure a uniform distribution of the inoculum on the cell monolayer. After incubation, the cells were overlaid with an agar overlay solution consisting of 50% of 2.5% carboxy methylcellulose (CMC) (Sigma), 50% 2× modified Eagle medium, 3% FBS, 1% penicillin-streptomycin, 1% L-glutamine, and 1% 1 M HEPES buffer (Mediatech) and incubated for 48 to 72 h at 37°C in a CO_2 incubator. Cells were then fixed with 4% paraformaldehyde for 24 h and counterstained with a 0.25% crystal violet solution in water, and viral plaques were counted.

Histological analysis. At 10 days postinfection, mice were sacrificed and perfused with 4% paraformaldehyde, pH 7.3. Excised tissues were embedded in paraffin, and 5-μm sections were prepared. To determine the extent of inflammation and tissue pathology, tissues were stained with hematoxylin and eosin (H&E) (39). Stained sections were blinded and scored for overall inflammatory cell infiltration and tissue damage as described previously (39). Both scoring systems utilized a 10-point scale where a score of 0 to 3 represents no to mild inflammation or damage, 4 to 6 represents moderate inflammation or damage, and 7 to 10 represents severe inflammation or damage. For the analysis of germinal center (GC) formation, spleen tissues from WT and $TLR7^{-/-}$ mice were stained with H&E, and stained sections were blinded and scored for the number of GCs and the number of total follicles within the section. GCs were identified within each follicle by their characteristic staining pattern of a pale, circular region surrounded by a darker region containing the mantle and marginal zones.

Flow cytometry. Mice were inoculated as described above, sacrificed by exsanguination at the indicated times postinfection, and perfused with 1× PBS. Quadriceps muscles or spleens were dissected, minced, and incubated for 1.5 to 2 h with vigorous shaking at 37°C in digestion buffer (RPMI, 10% fetal bovine serum, 15 mM HEPES, 2.5 mg/ml collagenase A [Worthington Biochemical Co.], 17 μg/ml DNase I [Roche]). Digested tissues were pelleted, resuspended in HFA buffer (Hanks balanced salt solution [Gibco], 1% fetal bovine serum, 0.1% sodium azide), passed through a 70-μm cell strainer, and centrifuged for 8 min at 1,000 rpm. Cells were resuspended in HFA buffer, and viable cell totals were determined by trypan blue exclusion. Isolated cells were incubated with various antibodies, according to the associated staining panel, for 30 min to 1 h at 4°C in fluorescence-activated cell sorter staining buffer (1× Hanks balanced salt solution, 1% fetal bovine serum, 2% normal rabbit serum). Cells were washed, fixed overnight in 2% paraformaldehyde, and analyzed on a Cyan cytometer (Becton Dickinson) using Summit software. Isolated splenocytes from mock-infected animals were prepared similarly and used for single-color staining controls. The lymphocyte staining panel included the following antibodies: anti-NK1.1–phycoerythrin (PE) (eBioscience), anti-CD3–fluorescein isothiocyanate (FITC) (eBioscience), anti-B220–PE Texas Red (PETR) (Invitrogen), anti-LCA–PECy5 (eBioscience), anti-F4/80–PECy7 (eBioscience), anti-CD4–Pacific blue (PB) (Caltag Laboratories), anti-CD8–Pacific orange (PO) (Invitrogen), anti-CD49b–allophycocyanin (APC) (eBioscience), and anti-GL7–Alexa 88 (eBioscience). The monocyte staining panel included the following antibodies: anti-Ly6G–FITC (BD Pharmingen), anti-SigLecF–PE (BD Pharmingen), anti-CD11c–PETR (Invitrogen), anti-LCA–PECy5 (eBioscience), anti-F4/80–PECy7 (eBioscience), anti-CD11b–eF450 (eBioscience), anti-major histocompatibility complex (MHC) class II–APC (eBioscience), and anti-B220–eF780 (eBioscience).

The gating strategies were as follows. For the inflammatory leukocytes, $CD11c^+$ LCA^+ viable cells were displayed on a histogram of Gr-1 plotted versus SigLecF. Neutrophils appear as a distinct Gr-1-high population, and $SigLecF^+$ cells appear on the other side of the diagonal. The $SigLecF^+$ subpopulation is displayed on a histogram of CD11b versus CD11c, where eosinophils appear as a CD11b-high, CD11c-low group, while resident macrophages are CD11b low and CD11c high. With neutrophils and SigLecF-high groups gated out, the remaining CD11c-positive cells are displayed on a plot of MHC class II versus B220. The B220-high, MHC class II-low plasmacytoid dendritic cells (pDCs) are gated out, and the remaining cells are displayed on a plot of MHC class II versus CD11b; the MHC class II-low cells are enumerated as monocyte-derived DCs (also referred to as TIP-DCs in some publications), and MHC class II-high, CD11b-high cells are classified as inflammatory DCs (or CD11b high DCs). For lymphocyte populations, viable lymphocytes (selected by forward/side scatter characteristics) are plotted on a histogram of CD3 versus autofluorescence, and the $CD3^+$ cells are further displayed on a plot of CD4 versus CD8. Lymphocytes that are both $CD19^+$ and $B220^+$ are counted as B cells, and those that are both $CD49b^+$ and $NK1.1^+$ are counted as NK cells.

Type I IFN (IFN-α/β) bioassay. Alpha/beta interferon (IFN-α/β) levels in cell culture supernatants were measured by an IFN bioassay as described previously (47, 48). Briefly, L929 mouse fibroblasts (ATCC CCL-1) were seeded into 96-well plates and grown in alpha minimal essential medium (αMEM). Samples were diluted 1:5 in αMEM, acidified to a pH of 2.0 for 24 h, and then neutralized to pH 7.4. Samples were then subjected to UV light for 15 min to inactivate any remaining virus, followed by titration of the samples by 2-fold serial dilutions across the seeded 96-well plate. Twenty-four hours later, encephalomyocarditis virus was added to each well at a multiplicity of infection (MOI) of 5. At 18 to 24 hpi, 3-(4,5-dimethyl-2-thiazolyl)-2,5-diphenyl-2H-tetrazolium bromide (MTT) (Sigma) was added to the plate to assess the viability in each well. The MTT product produced by viable cells was dissolved in isopropanol containing 0.4% hydrochloric acid and quantified by absorbance readings on a microplate reader at 570 nm. Each plate contained an IFN-β standard (Chemicon or R&D Systems) that was used to determine the number of international units of IFN-α/β per milliliter of the unknown samples.

PRNT assay. Neutralizing antibody titers were determined by plaque reduction neutralization test (PRNT) assay on Vero cell monolayers. Briefly, mouse sera were heat inactivated at 56°C for 30 min in a water bath and then placed on ice. Identical volumes (200 μl) of 2-fold mouse serum dilutions (1:2) and wild-type RRV (10^3 PFU virus/ml of PBS diluent) were

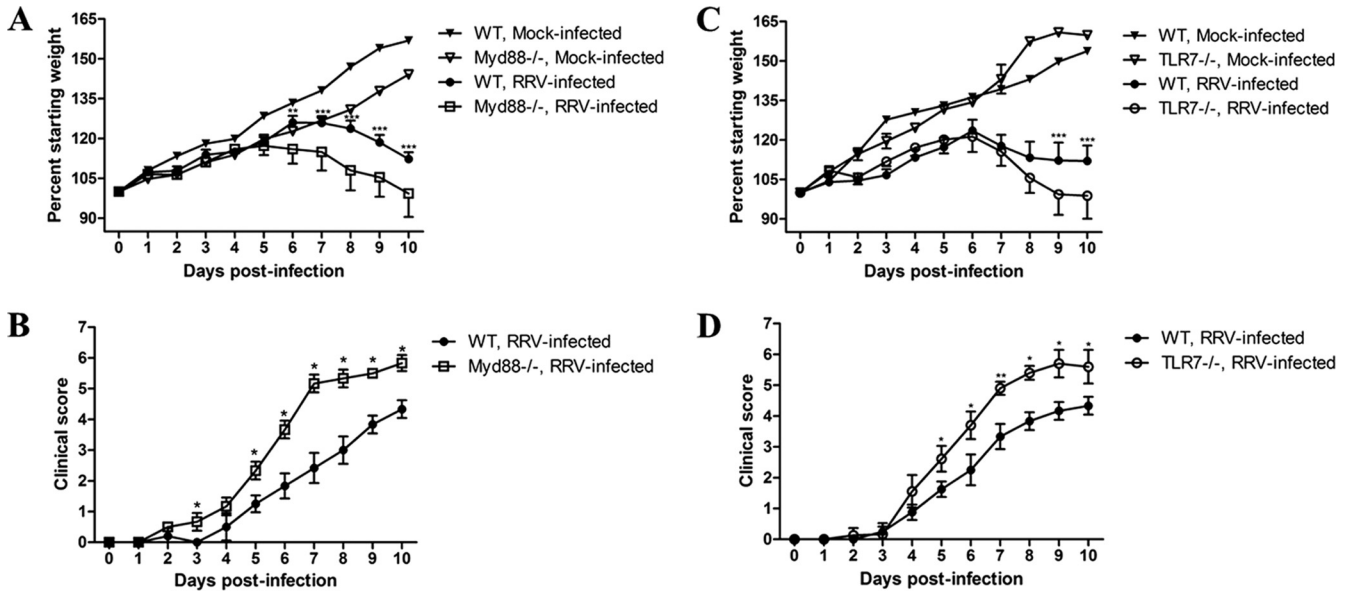

FIG 1 TLR7 and Myd88 contribute to protection from RRV-induced disease *in vivo*. Twenty-four-day-old C57BL/6J wild-type (WT), TLR7$^{-/-}$, and Myd88$^{-/-}$ mice were subcutaneously infected in the left rear footpad with either PBS diluent (mock) or 10^3 PFU of RRV and monitored for weight loss (A and C) and clinical disease (B and D) (n = 5 to 15 mice/strain/time point). *, $P < 0.01$; **, $P \leq 0.001$; and ***, $P \leq 0.0001$.

mixed together and incubated at 37°C for 30 min in a water bath. After incubation, 200 μl of serum-virus sample mixture was pipetted into each well of 70% confluent Vero cells in duplicate for each dilution. The samples were incubated on the cells for 1 h at 37°C in a CO_2 incubator and gently agitated every 15 min to ensure a uniform distribution of the inoculum on the cell monolayer. After incubation, the cells were overlaid with an agar overlay solution consisting of 50% 2.5% CMC (Sigma), 50% 2× modified Eagle medium, 3% FBS, 1% penicillin-streptomycin, 1% L-glutamine, and 1% 1 M HEPES buffer (Mediatech) and incubated for 48 to 72 h at 37°C in a CO_2 incubator. Cells were then fixed with 4% paraformaldehyde for 24 h and counterstained with a 0.25% crystal violet solution in water, and viral plaques were counted. Neutralizing antibody titers are expressed as $PRNT_{50}$, which is the reciprocal dilution where 50% of the total number of viral plaques in the virus-PBS diluent samples was reduced.

ELISA. RRV-specific antibody titers in sera of infected mice were determined by enzyme-linked immunosorbent assay (ELISA) with inactivated RRV (1 μg/ml) on high-binding 96-well plates. The serum was first diluted 20-fold and then further diluted in 2-fold serial dilutions. The ELISA antibody titer expressed is the estimated dilution factor that gave an optical density at 450 nm (OD_{450}) of 0.2 and is derived from nonlinear regression analysis of the serial dilution curve. Detection of bound antibody was done using a horseradish peroxidase (HRP)-conjugated goat anti-mouse secondary antibody (Abcam, Cambridge, MA) and ABTS [2,2′-azinobis(3-ethylbenzthiazolinesulfonic acid)] substrate (Invitrogen).

Antibody affinity ELISA. RRV-specific antibody titers in sera of WT and TLR7$^{-/-}$ infected mice were first determined by ELISA as described above. Inactivated RRV (1 μg/ml) was then plated on high-binding 96-well plates for 12 to 24 h, and serum was diluted in antibody diluent (PBS containing 0.05% Tween 20 and 10% Sigma Block) and then plated at a known dilution across the plate to obtain maximum antibody-antigen binding and incubated at 4°C for 2 h. Following the serum incubation, increasing concentrations of sodium thiocyanate (NaSCN) were added to the plate to serially dissociate the antibody-antigen complexes, followed by incubation with a conjugated secondary IgG antibody and substrate incubation as described in "ELISA" above. Values were reported as the percent maximum total IgG binding at each NaSCN concentration.

Passive serum transfer. Twenty-four-day-old WT and TLR7$^{-/-}$ mice were subcutaneously infected in the left rear footpad with 10^3 PFU of RRV and subsequently harvested at day 10 postinfection by exsanguination. Sera from each strain of infected mice were collected, pooled according to strain, and heat inactivated at 56°C for 1 h. Twenty-four-day-old naïve WT mice were then inoculated intraperitoneally with 50 μl of the heat-inactivated WT or TLR7$^{-/-}$ antisera. At 1 h after serum transfer, the mice were subcutaneously infected in the left rear footpad with 10^3 PFU of RRV and monitored daily for weight loss and disease signs as described above.

Statistical analyses. Data were analyzed using Prism software (GraphPad Software, Inc.). Comparisons of one-variable data were performed using a two-tailed unpaired Student t test. Percent starting weights for WT, TLR7$^{-/-}$, and Myd88$^{-/-}$ mice were analyzed using a one-way analysis of variance (ANOVA) with multiple-comparison corrections (a P value of <0.01 is considered significant). Clinical scores for WT, TLR7$^{-/-}$, and Myd88$^{-/-}$ mice were analyzed by Mann-Whitney analysis with Bonferroni's correction (a P value of <0.01 is considered significant). Bar graphs represent mean values ± standard deviations. Significant differences are represented as follows unless otherwise indicated: *, $P \leq 0.05$; **, $P \leq 0.01$; ***, $P \leq 0.001$; and ****, $P \leq 0.0001$.

RESULTS

Myd88 mediates protection from RRV-induced disease. Previous studies have shown that the host inflammatory response plays a major role in the pathogenesis of alphavirus-induced arthritis and myositis (21, 29–31, 37, 38). To further define the host pathways that contribute to alphavirus-induced pathology, we evaluated the role of Toll-like receptors (TLRs) in a mouse model of RRV-induced arthritis/myositis. Because Myd88 is an essential adaptor for signaling through multiple TLRs, we evaluated mice deficient in Myd88 for their susceptibility to RRV-induced inflammatory disease (42, 55, 60, 62). Myd88-deficient (Myd88$^{-/-}$) mice were highly susceptible to RRV-induced disease, with Myd88$^{-/-}$ mice developing more severe disease signs, as measured by weight loss and clinical disease scores, than wild-type (WT) C57BL/6J animals over the course of infection (Fig. 1A and B). Consistent with previous studies, RRV-infected WT mice lost weight between days 6 and 10 postinfection and reached peak disease scores between days 9 and 10 postinfection (Fig. 1A and B).

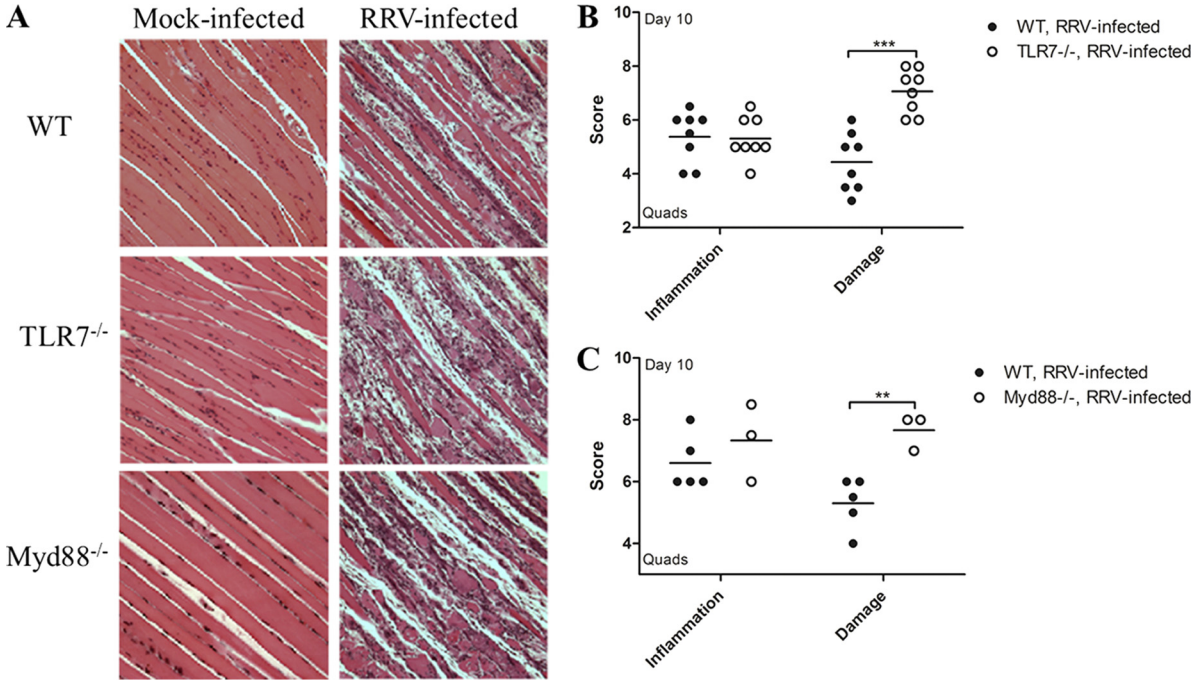

FIG 2 TLR7- and Myd88-deficient mice show enhanced tissue damage following RRV infection. Twenty-four-day old WT, TLR7$^{-/-}$, and Myd88$^{-/-}$ mice were subcutaneously infected in the left rear footpad with either PBS diluent or 10^3 PFU of RRV. Mice were sacrificed and perfused with 4% paraformaldehyde at 10 days postinfection. Quadriceps muscles were excised and paraffin embedded, and 5-μm tissue sections were stained with H&E. (A) Histological analysis of mock-infected and RRV-infected quadriceps muscles from WT, TLR7$^{-/-}$, and Myd88$^{-/-}$ mice at day 10 postinfection. Representative images are shown. (B) Blind scoring of overall inflammatory cell infiltration and damage observed in RRV-infected WT and TLR7$^{-/-}$ muscle tissue. ($n = 8$ for WT and TLR7$^{-/-}$). (C) Blind scoring of overall inflammatory cell infiltration and damage observed in RRV-infected WT and Myd88$^{-/-}$ muscle tissue ($n = 5$ [WT] or 3 [Myd88$^{-/-}$]). **, $P \leq 0.01$; ***, $P \leq 0.001$.

Although Myd88$^{-/-}$ mice showed a similar disease progression, they lost more weight and exhibited more severe disease than WT animals over the course of RRV infection (Fig. 1A and B). Furthermore, while RRV-induced disease is self-limited in WT animals, with the animals completely recovering from RRV-induced disease, 100% of Myd88$^{-/-}$ mice were moribund by day 10 postinfection and had to be euthanized. These results suggest that rather than contributing to disease pathogenesis, Myd88-dependent signaling plays an essential protective role during RRV infection.

TLR7-deficient mice exhibit a phenotype identical to that of Myd88-deficient animals. While Myd88 operates as an essential adaptor molecule for most TLRs, it can also serve as an adaptor for interleukin-1 (IL-1) and IL-18 receptor signaling (3, 7). Therefore, it was unclear whether Myd88's protective effect during RRV infection reflected a role for a specific TLR or possibly signaling through the IL-1/IL-18 receptors. To address this question, we sought to evaluate the roles of specific TLRs in the pathogenesis of RRV-induced disease. These studies initially focused on TLR7, a Myd88-dependent TLR that is known to play a role in the antiviral response against multiple viruses, including single-stranded RNA viruses (12, 32, 33, 49, 52, 62, 63). When TLR7$^{-/-}$ mice were infected with RRV, they exhibited a phenotype identical to that of Myd88-deficient animals, with TLR7$^{-/-}$ mice losing more weight and developing more severe disease signs than WT mice (Fig. 1C and D). RRV-infected WT and TLR7$^{-/-}$ mice lost weight between 7 and 10 days postinfection, with TLR7$^{-/-}$ mice losing weight at a higher rate than WT animals (Fig. 1C). WT and TLR7$^{-/-}$ mice reached peak clinical disease scores between days 9 and 10 days after RRV infection (Fig. 1D). However, mice deficient in TLR7 developed disease more rapidly than WT animals following RRV infection, and peak disease was more severe, with peak disease scores in TLR7$^{-/-}$ mice (5.7 ± 0.4) being significantly higher than disease scores in WT animals (4.3 ± 0.2) (Fig. 1D). Similar to the case for Myd88$^{-/-}$ mice, TLR7$^{-/-}$ mice became moribund by day 10 postinfection and had to be euthanized. Therefore, although we cannot rule out a role for other Myd88-dependent TLRs, such as TLR2, or IL-1/IL-18 receptor signaling in the pathogenesis of RRV infection, these results indicate that TLR7-dependent signaling through Myd88 plays a major protective role during RRV infection.

Tissue damage is enhanced in Myd88- and TLR7-deficient mice following RRV infection. Because skeletal muscle is a targeted tissue for viral replication, inflammation, and tissue destruction following RRV infection (37–39), we evaluated the roles of TLR7 and Myd88 in protection from RRV-induced tissue damage and inflammation. WT, TLR7$^{-/-}$, and Myd88$^{-/-}$ mice were sacrificed at 10 days postinfection, which represents the time of peak disease in the animals (37–39), and quadriceps tissues were excised and prepared for histological analysis. As shown in Fig. 2, TLR7$^{-/-}$ and Myd88$^{-/-}$ mice showed enhanced tissue damage in skeletal muscle tissue compared with WT mice following RRV infection. While mock-infected animals of all strains showed similar levels of resident inflammatory cells and intact muscle fibers in skeletal muscle tissue, muscle tissue from TLR7$^{-/-}$ and Myd88$^{-/-}$ mice showed fewer intact muscle fibers and more over-

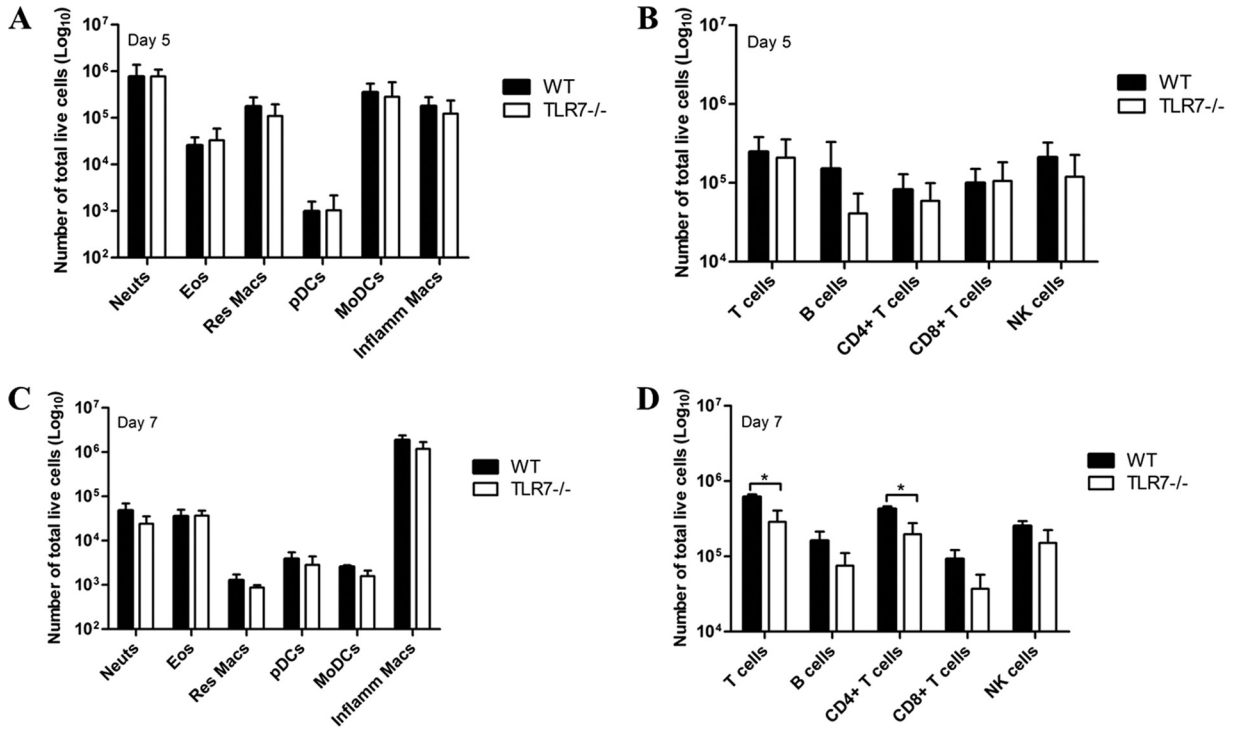

FIG 3 Inflammatory cell recruitment is similar in WT and TLR7$^{-/-}$ mice following RRV infection. Twenty-four-day-old WT and TLR7$^{-/-}$ mice were subcutaneously infected in the left rear footpad with 10^3 PFU of RRV. At 5 and 7 days postinfection, mice were sacrificed and perfused with 1× PBS. Quadriceps muscles were excised, digested, and prepared for flow cytometric analysis as described in Materials and Methods. (A and C) Total numbers of infiltrating inflammatory leukocyte cell populations isolated from RRV-infected WT and TLR7$^{-/-}$ quadriceps muscle tissue. (B and D) Total numbers of infiltrating lymphocyte cell populations isolated from RRV-infected quadriceps muscle tissue (n = 4 to 7 mice/strain/time point). *, $P \leq 0.01$.

all tissue destruction following RRV infection than that from WT mice, despite similar levels of inflammation (Fig. 2A).

To quantify the extent of inflammation and damage present in the muscle tissues at 10 days postinfection, histological slides were blinded and scored using a blind scoring method that assigns scores based on the presence of inflammatory cell infiltrates and overall damage in the muscle tissue (Fig. 2B and C). The results of the blind scoring analyses showed that while WT and TLR7$^{-/-}$ mice showed similar levels of inflammatory cell infiltration in skeletal muscle tissue following RRV infection, there was significantly more damage in the quadriceps tissue of TLR7$^{-/-}$ mice than in that of WT mice (Fig. 2B), and this was also observed following histological scoring of WT and Myd88$^{-/-}$ skeletal muscle tissues (Fig. 2C). However, no differences were observed following histological analyses of nontarget tissues, such as the brain and spinal cord, of WT, TLR7$^{-/-}$, and Myd88$^{-/-}$ mice at day 10 postinfection (data not shown), suggesting that the enhanced tissue damage observed in TLR7- and Myd88-deficient mice is specific to RRV-targeted skeletal muscle. These data suggest that TLR7 and Myd88 play a critical role in protection from severe skeletal muscle damage following RRV infection.

TLR7 deficiency does not affect macrophage recruitment but does affect T cell recruitment into RRV-infected muscle tissue. Previous studies have shown that inflammatory macrophages play a major role in promoting RRV-induced disease (21, 30, 31). Although the histological scoring analyses revealed similar degrees of inflammation in the skeletal muscle tissue of WT and TLR7$^{-/-}$ mice following RRV infection, we sought to more rigorously quantify the overall number and composition of inflammatory cells within the skeletal muscle of RRV-infected TLR7$^{-/-}$ and WT mice. At 5 and 7 days postinfection, WT and TLR7$^{-/-}$ mice showed similar numbers of inflammatory leukocyte cell populations, including inflammatory macrophages, in RRV-infected quadriceps tissues as determined by flow cytometry (Fig. 3A and C). Moreover, total numbers of LCA-positive cells isolated from RRV-infected muscle tissues were not different in WT and TLR7$^{-/-}$ mice at both 5 and 7 days postinfection (data not shown). Analyses of infiltrating lymphocytes in the quadriceps muscle tissues revealed a slight decrease in the total numbers of lymphocyte cell populations, including B cells and CD4$^+$ T cells, in TLR7$^{-/-}$ mice compared to WT mice at 5 and 7 days after RRV infection (Fig. 3B and D). Additionally, there was a small but statistically significant decrease in CD3-positive and CD4-positive T cell populations within TLR7$^{-/-}$ mice relative to WT mice at 7 days postinfection (Fig. 3D). Therefore, although TLR7 deficiency did not have a general effect on inflammatory cell recruitment, it appears that TLR7 deficiency does affect T cell recruitment into the inflamed muscle tissue during RRV infection.

Type I IFN production in sera of TLR7- and Myd88-deficient mice is similar to that in sera of WT mice at early times after RRV infection. TLR7 is known to play an important role in the antiviral response against a wide range of viral pathogens, in large part through its ability to regulate type I IFN responses (8, 14, 32, 54, 64, 66). Because type I IFN receptor signaling is essential for the control of a number of alphaviruses (5, 11, 16, 45, 61), including RRV (R. Shabman and M. T. Heise, unpublished data), we

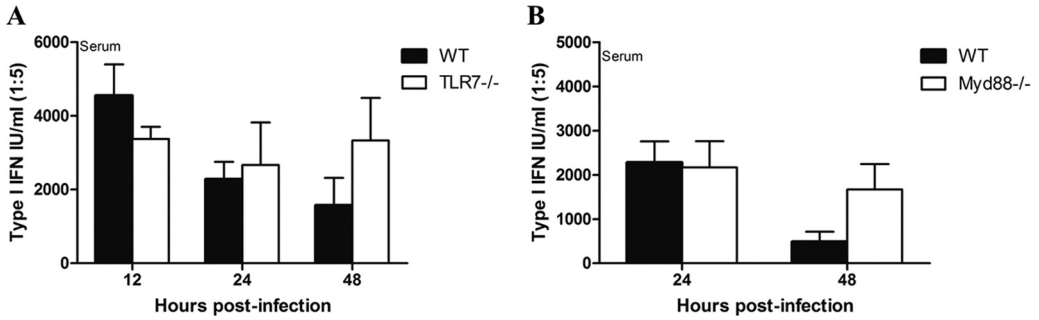

FIG 4 Type I IFN production in sera of TLR7$^{-/-}$ and Myd88$^{-/-}$ mice is similar to that in sera of WT mice early during infection. Twenty-four-day-old WT, TLR7$^{-/-}$, and Myd88$^{-/-}$ mice were subcutaneously infected in the left rear footpad with 10^3 PFU of RRV. At the indicated time points, mice were sacrificed by exsanguination and serum was collected. Serum was diluted 1:5 in medium and analyzed for the presence of type I IFN (IFN-α/β) by IFN bioassay as described in Materials and Methods. (A) Type I IFN production in sera of WT and TLR7$^{-/-}$ mice. (B) Type I IFN production in sera of WT and Myd88$^{-/-}$ mice ($n = 3$ to 5 mice/strain/time point).

evaluated whether TLR7 was required for the early regulation of type I IFN responses *in vivo*. As shown in Fig. 4, there were no differences in type I IFN production between WT and TLR7-deficient animals at 12, 24, and 48 h postinfection as measured by type I IFN bioassay (Fig. 4A). Moreover, type I IFN production was similar in WT and Myd88$^{-/-}$ mice at 24 and 48 h postinfection (Fig. 4B), suggesting that the early type I IFN response does not contribute to the enhanced disease phenotype observed in TLR7- and Myd88-deficient mice following RRV infection.

Viral titers are elevated in mice lacking TLR7 or Myd88 at late times postinfection. To determine whether the viral burden was altered in mice deficient in TLR7 or Myd88, we quantified the amount of virus present in the quadriceps muscles and sera of WT, TLR7$^{-/-}$, and Myd88$^{-/-}$ mice at various times after RRV infection. No significant differences in viral titer were detected in the quadriceps muscles or sera of WT, TLR7$^{-/-}$, and Myd88$^{-/-}$ mice at early times postinfection (Fig. 5). WT and TLR7$^{-/-}$ mice did not show significant differences in viral titer in the quadriceps muscles by plaque assay at days 0.5, 1, 2, and 3 postinfection (Fig. 5A). However, viral titers in the sera of TLR7$^{-/-}$ mice were significantly enhanced over those in WT mice at day 3 postinfection (Fig. 5B), and analysis of the viral burden in infected quadriceps tissues at later times postinfection revealed that TLR7$^{-/-}$ mice had significantly higher viral titers than WT mice at days 5 and 7 postinfection (Fig. 5A). Similar results were found in Myd88-deficient mice (Fig. 5C and D). Viral titers in the quadriceps were similar at day 10 postinfection in WT, TLR7$^{-/-}$, and Myd88$^{-/-}$ mice (Fig. 5A and C), with all samples being close to or below the limit of viral detection. Therefore, these findings suggest that RRV is able to infect and spread within target tissues of TLR7$^{-/-}$ and Myd88$^{-/-}$ mice with kinetics similar to those in WT animals early during infection, but mice lacking TLR7 or Myd88 exhibit delayed control of viral replication within the muscle tissue at later times postinfection. Although RRV-induced disease is characterized by

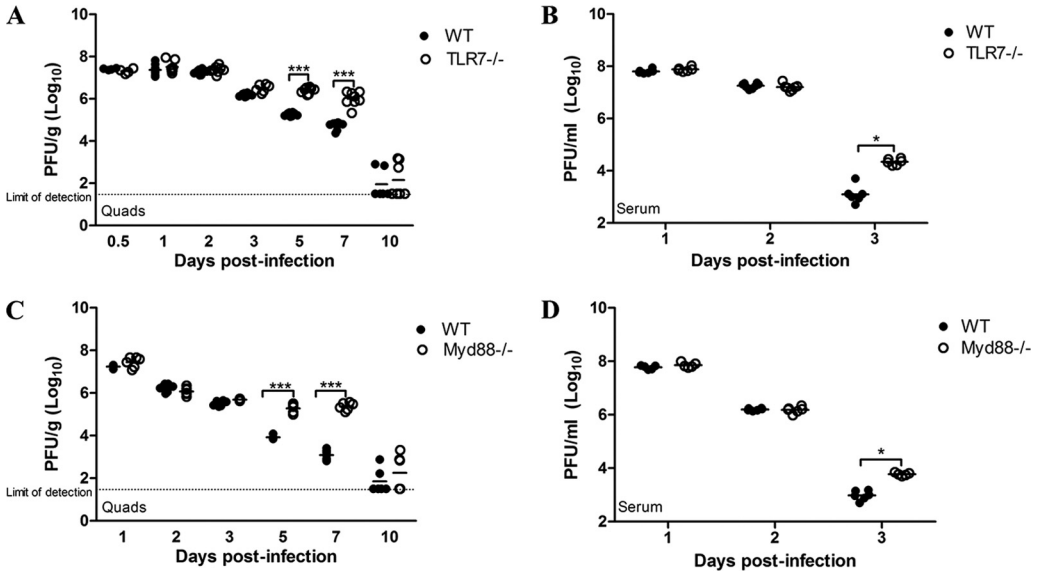

FIG 5 Mice lacking TLR7 or Myd88 show an inability to control viral titer at late times postinfection. Twenty-four-day-old WT, TLR7$^{-/-}$, and Myd88$^{-/-}$ mice were subcutaneously infected in the left rear footpad with 10^3 PFU of RRV. At the indicated time points, mice were sacrificed by exsanguination and quadriceps tissues were dissected. Infectious virus present in homogenized ipsilateral quadriceps tissue (A and C) and serum (B and D) was quantified by plaque assay on Vero cells ($n = 4$ to 8 mice/strain/time point). *, $P \leq 0.05$; **, $P \leq 0.01$; ***, $P \leq 0.001$.

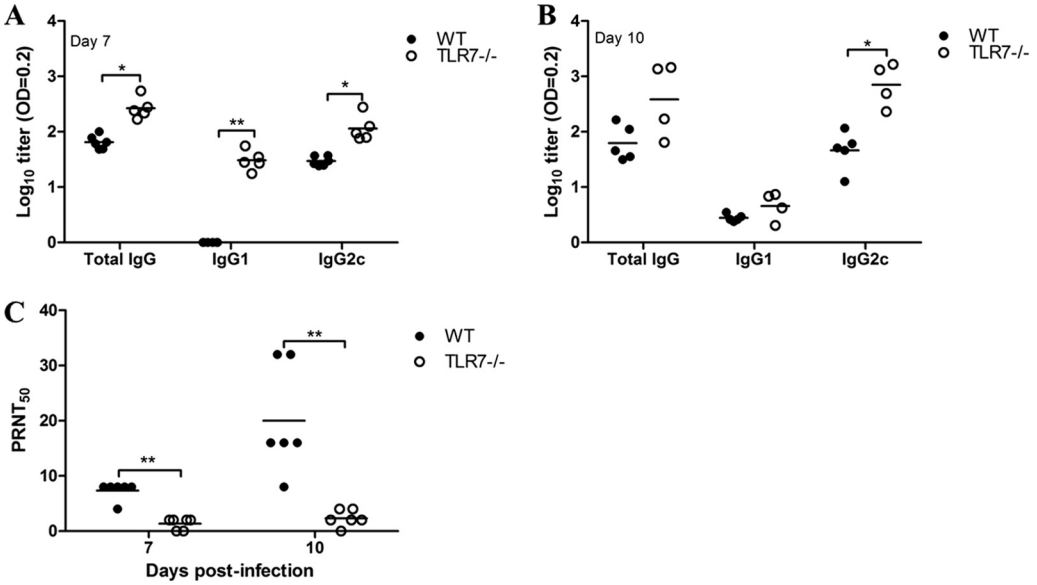

FIG 6 TLR7$^{-/-}$ mice show reduced neutralizing antibody production following RRV infection. Twenty-four-day-old WT and TLR7$^{-/-}$ mice were subcutaneously infected in the left rear footpad with 10^3 PFU of RRV. (A and B) At 7 and 10 days postinfection, mice were sacrificed by exsanguination and serum antibody levels were measured by ELISA as described in Materials and Methods. Levels of total RRV-specific IgG, IgG1, and IgG2c antibodies in RRV-infected WT and TLR7$^{-/-}$ mice at day 7 (A) and day 10 (B) are shown. (C) At 7 and 10 days postinfection, mice were sacrificed by exsanguination and sera from RRV-infected WT and TLR7$^{-/-}$ mice was tested for RRV neutralization activity using PRNT assay as described in Materials and Methods. Neutralizing antibody titers are expressed as the inverse of the dilution where 50% of the virus present was neutralized ($PRNT_{50}$) for a given sample ($n = 6$ mice/strain/time point). *, $P \leq 0.05$; **, $P \leq 0.01$; and ***, $P \leq 0.001$.

high levels of viral replication within joint and muscle tissues, with subsequent overactive inflammatory responses in these tissues contributing to disease pathogenesis (31, 37–39), the inability of TLR7- or Myd88-deficient mice to control viral replication at late times postinfection raised the possibility that the enhanced disease/mortality in these mice might be due to enhanced viral replication in other tissues, such as the central nervous system (CNS). However, we observed no differences in viral load within the brains and spinal cords of WT and TLR7$^{-/-}$ mice at 1 and 2 days postinfection, and viral titers in these tissues were below the limit of detection for both mouse strains by day 7 postinfection (data not shown). We also observed no differences in viral titer in the kidneys, livers, spleens, and draining lymph nodes between WT and TLR7$^{-/-}$ mice at 1 and 2 days postinfection (data not shown), suggesting that excess viral replication within the CNS or other tissues that are not targets of RRV infection does not explain the enhanced disease observed in TLR7-deficient mice.

TLR7$^{-/-}$ mice show reduced neutralizing antibody production and decreased antibody affinity following RRV infection. Because TLR7$^{-/-}$ mice showed enhanced viral titers compared to WT mice at late times postinfection, we hypothesized that deficiency in TLR7 signaling may result in an ineffective antibody response that leads to an inability to control viral replication during RRV infection. To determine whether deficiency in TLR7 affected antibody production following RRV infection, RRV-specific antibody levels in the sera of WT and TLR7$^{-/-}$ mice were quantified by ELISA at 7 and 10 days postinfection (Fig. 6A and B). TLR7$^{-/-}$ mice showed increased RRV-specific total IgG production at 7 and 10 days postinfection compared with WT animals (Fig. 6A and B), with TLR7$^{-/-}$ mice having significantly increased total RRV-specific IgG at day 7 postinfection (Fig. 6A). Additionally, analysis of RRV-specific IgG subtypes revealed that TLR7$^{-/-}$ mice showed significantly increased IgG1 and IgG2c antibody production at 7 days postinfection, as well as increased IgG2c antibody levels at day 10 postinfection, relative to WT mice (Fig. 6A and B). These results suggest that RRV-specific antibody production is elevated in TLR7$^{-/-}$ mice following RRV infection. Furthermore, because IgG1 is indicative of T-helper 2 (Th2) immune responses and IgG2c is indicative of T-helper 1 (Th1) immunity, analysis of RRV-specific IgG subtypes reveals that TLR7$^{-/-}$ mice have a skewed Th1/Th2 antibody response following RRV infection relative to WT mice (Fig. 6A and B) (40, 41, 43).

To determine whether the quality of RRV-specific antibody was altered in TLR7-deficient mice, we first tested the neutralization capacities of WT and TLR7$^{-/-}$ antisera from 7 and 10 days after RRV infection by PRNT assay (Fig. 5C). Antisera from TLR7$^{-/-}$ mice had significantly less neutralization activity than WT antisera at both 7 and 10 days postinfection, suggesting that the quality of RRV-specific antibody produced by TLR7-deficient mice is defective and it is less neutralizing than WT antibody responses following RRV infection (Fig. 6C). To further assess the quality of RRV-specific antibody in TLR7$^{-/-}$ mice, we determined whether TLR7 deficiency altered the affinity of RRV-specific antibody using an affinity ELISA (Fig. 7A). As shown in Fig. 7, RRV-specific IgG from infected TLR7$^{-/-}$ mice displayed less affinity for RRV than WT IgG, suggesting that TLR7 deficiency affects the affinity maturation of virus-specific antibody during RRV infection.

Lastly, we directly tested whether sera from RRV-infected TLR7$^{-/-}$ mice showed a reduced capacity to protect from RRV-induced disease in adoptive transfer studies. We passively transferred heat-inactivated sera obtained from WT or TLR7$^{-/-}$ mice at day 10 postinfection to naïve WT mice prior to RRV infection. As shown in Fig. 7, the transfer of TLR7-deficient antisera failed to

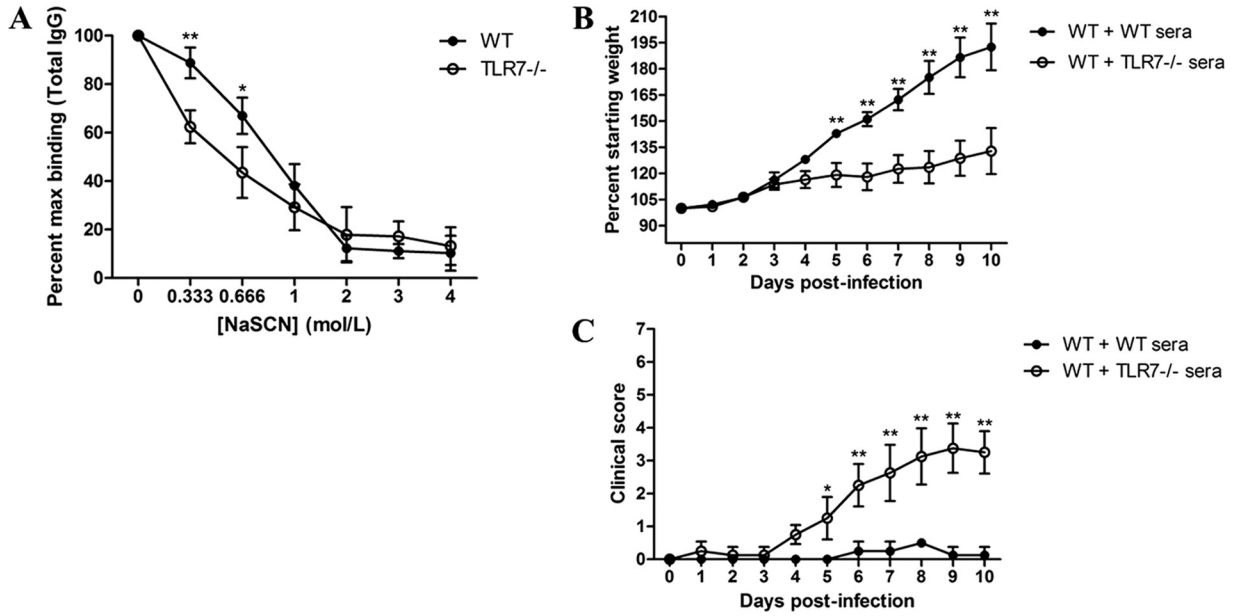

FIG 7 Antibody from TLR7$^{-/-}$ mice shows decreased virus-specific affinity and fails to protect from RRV-induced disease. Twenty-four-day-old WT and TLR7$^{-/-}$ mice were subcutaneously infected in the left rear footpad with 10^3 PFU of RRV. At 10 days postinfection, mice were sacrificed by exsanguination and serum antibody levels were measured by ELISA as described in Materials and Methods. (A) To measure antibody affinity, inactivated RRV was plated on ELISA plates and sera were added at a 1:40 dilution across the plate. Levels of total IgG were measured in the presence of increasing concentrations of NaSCN as described in Materials and Methods. Representative data are shown, where $n = 4$ (WT) or 6 (TLR7$^{-/-}$) mice. (B and C) Twenty-four-day-old WT mice were intraperitoneally inoculated with 50 μl of heat-inactivated sera from RRV-infected WT or TLR7$^{-/-}$ mice harvested at day 10 postinfection. At 1 h after serum transfer, mice were subcutaneously infected in the left rear footpad with 10^3 PFU of RRV and monitored for weight loss (B) and clinical disease (C) ($n = 4$ mice/group/time point). *, $P \leq 0.001$; **, $P \leq 0.0001$.

protect WT mice from RRV infection (Fig. 7B and C). WT mice that received sera from RRV-infected TLR7$^{-/-}$ mice showed significantly reduced weight gain and enhanced disease signs between days 5 and 10 postinfection compared to mice that received WT antisera, which were protected from RRV-induced disease (Fig. 7B and C).Taken together, these results indicate that TLR7 is critically important in the establishment of an effective antibody response following RRV infection.

Myd88 and TLR7 deficiency alters germinal center development following RRV infection. Germinal center (GC) B cells have been shown to be critical for antibody affinity maturation and for the development of class-switched neutralizing antibodies (1). Because RRV-specific antibody responses were defective in TLR7-deficient mice, we investigated whether GC development was altered in TLR7$^{-/-}$ mice during RRV infection. As shown in Fig. 8, histological analysis of spleens from WT and TLR7$^{-/-}$ mice at day 10 postinfection revealed that TLR7$^{-/-}$ mice had reduced GC formation following RRV infection. While RRV-infected WT mice exhibited abundant GC structures at 10 days postinfection, GC formation was visibly reduced in TLR7$^{-/-}$ mouse spleens (Fig. 8A). Blind scoring analysis of GC formation also revealed a reduced percentage of GCs per follicle in TLR7-deficient mice (Fig. 8B). To determine whether Myd88-dependent TLR7 signaling is important in GC B cell development, we quantified the total numbers of GC B cells present in the spleens of WT and Myd88$^{-/-}$ mice at day 9 after RRV infection by flow cytometry. As shown in Fig. 8C, Myd88-deficient mice showed significantly reduced GL7^{+} GC B cells compared to WT mice. These results demonstrate that Myd88-dependent TLR7 signaling is critical for germinal center development and further indicate the importance of TLR7 in generating an effective adaptive immune response during RRV infection.

DISCUSSION

The host inflammatory response is known to play a major role in the pathogenesis of alphavirus-induced arthritis and myositis, yet the roles of specific host sensing pathways in regulating these processes have not been investigated in detail. The studies presented here demonstrate that TLR7 and its essential adaptor molecule, Myd88, mediate protection against severe RRV-induced disease and mortality. Furthermore, both TLR7- and Myd88-deficient mice exhibited a defect in viral clearance, and TLR7$^{-/-}$ mice failed to mount effective antibody responses against RRV, showing both reduced antibody neutralizing activity and reduced RRV-specific antibody affinity. Moreover, TLR7$^{-/-}$ mice show reduced germinal center formation and Myd88-deficient mice show reduced germinal center (GL7^{+}) B cells compared to those of WT animals following RRV infection. These results suggest that TLR7-dependent interactions with the adaptive immune response play a crucial role in regulating the development of protective immune responses against RRV. Although we cannot rule out a role for other Myd88-dependent TLRs, such as TLR2, or IL-1/IL-18 receptor signaling in RRV-induced disease, these findings provide new insights into the role that TLR7 plays in alphavirus pathogenesis by highlighting the importance of this pathway in regulating antiviral adaptive immunity and by identifying TLR7 as a possible target for enhancing vaccine-induced immune responses against alphaviruses.

To our knowledge, TLR7's role in alphavirus pathogenesis has not previously been investigated. Because type I IFN receptor sig-

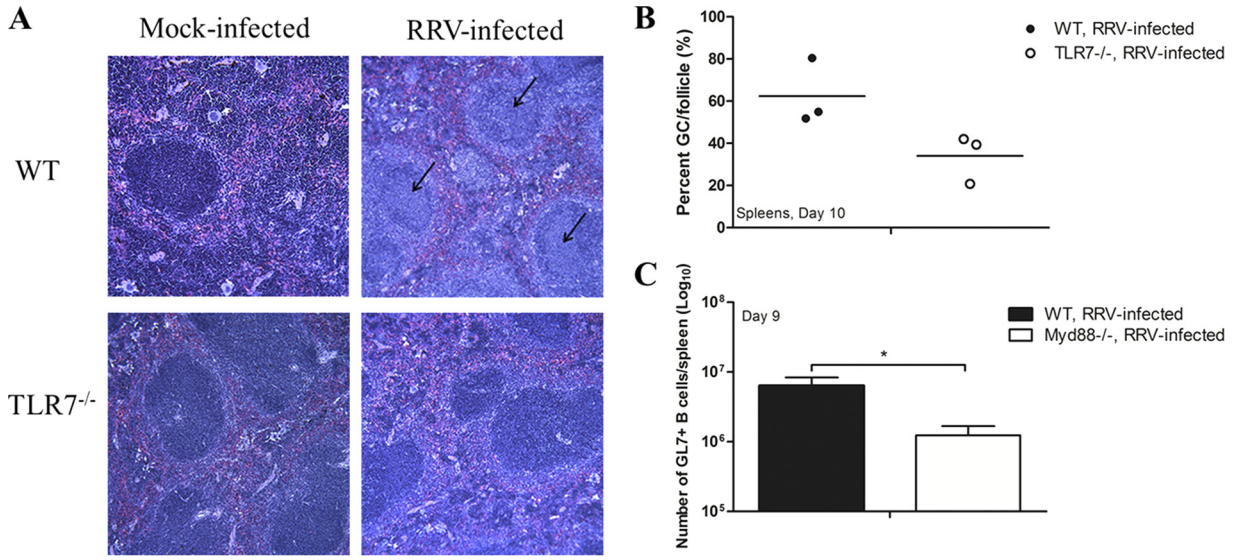

FIG 8 TLR7$^{-/-}$ mice show reduced germinal center formation following RRV infection. Twenty-four-day-old WT and TLR7$^{-/-}$ mice were subcutaneously infected in the left rear footpad with 10^3 PFU of RRV. Mice were sacrificed and perfused with 4% paraformaldehyde at 10 days postinfection. Spleens were excised and paraffin embedded, and 5-μm tissue sections were stained with H&E. (A) Histological analysis of mock-infected and RRV-infected spleens from WT and TLR7$^{-/-}$ mice at day 10 postinfection. Representative images are shown. (B) Blind scoring of germinal centers (GCs) per follicle observed in WT and TLR7$^{-/-}$ spleens. GCs are indicated by arrows ($n = 3$ mice/strain). (C) Twenty-four-day-old WT and Myd88$^{-/-}$ mice were subcutaneously infected in the left rear footpad with 10^3 PFU of RRV At 9 days postinfection, mice were sacrificed and perfused with 1× PBS. Spleens were excised and prepared for flow cytometric analysis as described in Materials and Methods. Total numbers of GL7$^+$ B cells isolated from RRV-infected WT and Myd88$^{-/-}$ mouse spleens are shown ($n = 5$ mice/strain). *, $P \leq 0.01$.

naling is important for the control of a number of alphaviruses (5, 11, 16, 45, 61), we initially focused our analysis on evaluating whether TLR7 was required for the early control of RRV infection or regulation of the type I IFN response *in vivo*. Somewhat surprisingly, we found no evidence for altered viral loads in either the serum or skeletal muscle at very early to intermediate times in the infection process (Fig. 5), nor did we find evidence for enhanced viral replication in other sites, such as the CNS and other nontarget tissues, that might contribute to exacerbated RRV-induced disease and mortality (data not shown). Furthermore, we found no evidence that systemic type I IFN responses were decreased in TLR7- and Myd88-deficient animals at early times postinfection as measured by type I IFN bioassay (Fig. 4), suggesting that other innate sensing pathways, such as RIG-I and protein kinase R (PKR), that are known to be involved in the type I IFN response to alphaviruses (2, 6, 44, 46), rather than TLR7, may contribute to the early antiviral response against RRV.

In contrast to our findings that TLR7 was not required for the early control of RRV replication, we did see significant defects in the ability of both TLR7- and Myd88-deficient animals to control RRV replication at late times postinfection. Moreover, although TLR7$^{-/-}$ mice were able to mount RRV-specific antibody responses, the virus-specific antibody that was produced demonstrated little neutralizing activity and showed less affinity for RRV than WT antibody, and TLR7- and Myd88-deficient mice exhibited defects in germinal center formation. Moreover, the passive transfer of TLR7-deficient antisera failed to protect naïve WT mice from *de novo* RRV infection, suggesting that TLR7 plays a major role in driving the development of protective antibody in response to RRV. Because Myd88-dependent TLR7 signaling in B cells has been shown to be important in the development of neutralizing antibodies during retrovirus infection (4), it is possible that TLR7 signaling is necessary for an effective antibody response to multiple viral pathogens. In addition to the impact on neutralizing antibody responses, we also found that TLR7 deficiency resulted in a reduction in the number of CD4$^+$ T cells recruited into the inflamed muscle tissue (Fig. 3). This observed decrease in T cell recruitment was not due to a general defect in inflammatory cell infiltration in the TLR7$^{-/-}$ mice, because macrophage recruitment was unaffected. Taken together, these findings provide further evidence that Myd88-dependent TLR7 signaling plays a role in regulating multiple aspects of the host adaptive immune response.

Although it remains to be determined exactly how TLR7 and MyD88 modulate RRV-induced adaptive immune responses, Myd88 has been shown to be required for efficient cross-presentation of viral antigens by dendritic cells, where Myd88 deficiency leads to decreased priming and activation of CD8-positive T cells during infection (9). Likewise, stimulation of TLR7 signaling during vaccination can improve neutralizing antibody production, and it is possible that TLR7 deficiency may also affect neutralizing activity and affinity maturation of antibodies during alphavirus infection (25). Importantly, given TLR7's importance in regulating the development of protective anti-RRV responses, these studies suggest that enhancing TLR7-mediated responses may be beneficial during vaccination against RRV or other alphaviruses.

TLR7 is expressed on a wide variety of cell types, including macrophages and dendritic cell subsets. Although type I IFN responses in many cell types, including myeloid dendritic cells, are independent of Myd88 and therefore TLR7 (15), TLR7 is the major driver of type I IFN production by plasmacytoid dendritic cell (pDCs) in response to viral infection or RNA ligands (18). Because pDCs are known to express high levels of TLR7 and have been shown to recognize single-stranded RNA (ssRNA) viruses

through TLR7 and Myd88, one potential mechanism for the enhanced RRV-induced disease seen in TLR7-deficient mice is through dysfunctional pDC activity (9, 10, 12, 18). We found no defect in the ability of pDCs isolated from TLR7-deficient mice to produce type I IFN in response to RRV infection *in vitro* (data not shown), although it is possible that pDCs lacking TLR7 may have other functional defects during RRV infection that we have not yet uncovered with our studies. Moreover, as noted above, a recent study demonstrated the importance of Myd88-dependent TLR7 signaling in B cells for the development of effective neutralizing antibody production during Friend virus infection (4), and it is possible that Myd88 and TLR7 deficiency in B cells may affect neutralizing antibody production during alphavirus infection as well. Studies are ongoing in our lab to assess whether TLR7 expression is required for the functional activity of pDCs, B cells, and other immune cell types in response to RRV infection.

These studies clearly demonstrate that TLR7 is required for protection from lethal RRV-induced disease and that TLR7 modulated the development of RRV-specific adaptive immune responses. However, it is not clear whether the delayed clearance of RRV infection in TLR7-deficient mice can be directly linked to the enhanced disease and virus-induced mortality. We have previously shown that RAG-1-deficient (RAG-1$^{-/-}$) mice, which lack functional T and B cells, are susceptible to RRV-induced disease (39). However, unlike TLR7-deficient animals, RAG-1$^{-/-}$ mice do not die from RRV-induced disease (39). This suggests that the lack of a protective adaptive immune response does not predispose mice to RRV-induced mortality. This raises two major possibilities. The first is whether TLR7 is regulating some aspect of early virus control, such as type I IFN responses, that we were unable to detect in our studies. While we cannot rule this possibility out, the fact that we did not observe any major changes in viral load at early times postinfection argues against this possibility. It is also possible that some aspect of the nonprotective adaptive immune response in TLR7$^{-/-}$ animals acts to exacerbate RRV-induced disease. A similar outcome has been found with respiratory syncytial virus (RSV) vaccination, where the lack of Myd88 signaling in response to RSV vaccination results in the lack of a protective anti-RSV response within the lungs and leads to the development of vaccine-induced immune pathology (13). This may be particularly important for RRV, because accumulation of immune complexes comprised of antibody-bound viral particles in TLR7-deficient animals could lead to enhanced complement activation via the classical pathway (56, 58). RRV-mediated inflammatory disease has previously been shown to be mediated by complement activation in a mouse model of infection, and other arthritic diseases are associated with complement activation as well (22, 24, 37, 38). Alternatively, the high titers of nonneutralizing, RRV-specific antibodies present in TLR7-deficient mice could enhance RRV infection through an antibody-dependent enhancement (ADE) mechanism, resulting in increased Fc-mediated uptake of antibody-bound viral particles by phagocytic cells (53). ADE has previously been reported to enhance RRV infection of macrophages *in vitro*, and this mechanism could explain the increased viral titers observed in TLR7- and Myd88-deficient animals at late times after RRV infection, correlating with the onset of adaptive immune responses (29). Studies are under way to determine whether either of these possible mechanisms contributes to the enhanced disease and mortality observed in RRV-infected TLR7$^{-/-}$ mice.

In conclusion, the results of this study identify an essential protective role for the Myd88-dependent TLR7 signaling pathway during RRV infection and further define the impact of host factors in the pathogenesis of alphavirus-induced arthritis/myositis. Given the impact of TLR7 signaling on viral control and on the generation of protective adaptive immunity following RRV infection, it may be beneficial to design vaccination and treatment strategies for alphavirus infections that enhance Myd88-dependent TLR7 signaling, such as through the delivery of TLR7 agonists or through stimulation of downstream signaling molecules, to ensure optimal protection from alphavirus-induced disease. Further studies will be necessary to elucidate the mechanism of TLR7-mediated protection from severe RRV-induced disease.

ACKNOWLEDGMENTS

This work was supported by NIH/NIAMS research grant R01 AR 047190 awarded to M.T.H. and by a Department of Defense-funded National Defense Science and Engineering Graduate (NDSEG) Fellowship awarded to L.M.N.

We thank the current and former members of the Carolina Vaccine Institute for their contributions through scientific discussions and through providing experimental protocols. We especially thank Tem Morrison for his early contributions in piloting experiments with the Myd88-deficient animals. Additionally, we thank Martin Ferris for assistance with statistical analyses and Bianca Trollinger for assistance with cell culture and mouse genotyping. We also thank the LCCC/DLAM histopathology core facility, the UNC flow cytometry core facility, and the UNC microscopy facility at UNC, Chapel Hill.

REFERENCES

1. **Aydar Y, Sukumar S, Szakal AK, Tew JG.** 2005. The influence of immune complex-bearing follicular dendritic cells on the IgM response, Ig class switching, and production of high affinity IgG. J. Immunol. **174**:5358–5366.
2. **Barry G, et al.** 2009. PKR acts early in infection to suppress Semliki Forest virus production and strongly enhances the type I interferon response. J. Gen. Virol. **90**:1382–1391.
3. **Boraschi D, Tagliabue A.** 2006. The interleukin-1 receptor family. Vitam. Horm. **74**:229–254.
4. **Browne EP.** 2011. Toll-like receptor 7 controls the anti-retroviral germinal center response. PLoS Pathog. 7:e1002293. doi:10.1371/journal.ppat.1002293.
5. **Burdeinick-Kerr R, Wind J, Griffin DE.** 2007. Synergistic roles of antibody and interferon in noncytolytic clearance of Sindbis virus from different regions of the central nervous system. J. Virol. **81**:5628–5636.
6. **Burke CW, Gardner CL, Steffan JJ, Ryman KD, Klimstra WB.** 2009. Characteristics of alpha/beta interferon induction after infection of murine fibroblasts with wild-type and mutant alphaviruses. Virology **395**:121–132.
7. **Burns K, et al.** 1998. MyD88, an adapter protein involved in interleukin-1 signaling. J. Biol. Chem. **273**:12203–12209.
8. **Cervantes-Barragan L, et al.** 2007. Control of coronavirus infection through plasmacytoid dendritic-cell-derived type I interferon. Blood **109**:1131–1137.
9. **Chen M, Barnfield C, Naslund TI, Fleeton MN, Liljestrom P.** 2005. MyD88 expression is required for efficient cross-presentation of viral antigens from infected cells. J. Virol. **79**:2964–2972.
10. **Colonna M, Trinchieri G, Liu YJ.** 2004. Plasmacytoid dendritic cells in immunity. Nat. Immunol. **5**:1219–1226.
11. **Couderc T, et al.** 2008. A mouse model for Chikungunya: young age and inefficient type-I interferon signaling are risk factors for severe disease. PLoS Pathog. **4**:e29. doi:10.1371/journal.ppat.0040029.
12. **Davidson S, et al.** 2011. Plasmacytoid dendritic cells promote host defense against acute pneumovirus infection via the TLR7-MyD88-dependent signaling pathway. J. Immunol. **186**:5938–5948.
13. **Delgado MF, et al.** 2009. Lack of antibody affinity maturation due to poor Toll-like receptor stimulation leads to enhanced respiratory syncytial virus disease. Nat. Med. **15**:34–41.

14. **Diebold SS, Kaisho T, Hemmi H, Akira S, CReis e Sousa.** 2004. Innate antiviral responses by means of TLR7-mediated recognition of single-stranded RNA. Science **303**:1529–1531.
15. **Diebold SS, et al.** 2003. Viral infection switches non-plasmacytoid dendritic cells into high interferon producers. Nature **424**:324–328.
16. **Fragkoudis R, et al.** 2007. The type I interferon system protects mice from Semliki Forest virus by preventing widespread virus dissemination in extraneural tissues, but does not mediate the restricted replication of avirulent virus in central nervous system neurons. J. Gen. Virol. **88**:3373–3384.
17. **Fraser JR.** 1986. Epidemic polyarthritis and Ross River virus disease. Clin. Rheum. Dis. **12**:369–388.
18. **Gilliet M, Cao W, Liu YJ.** 2008. Plasmacytoid dendritic cells: sensing nucleic acids in viral infection and autoimmune diseases. Nat. Rev. Immunol. **8**:594–606.
19. **Gould EA, et al.** 2010. Understanding the alphaviruses: recent research on important emerging pathogens and progress towards their control. Antiviral Res. **87**:111–124.
20. **Harley D, Sleigh A, Ritchie S.** 2001. Ross River virus transmission, infection, and disease: a cross-disciplinary review. Clin. Microbiol. Rev. **14**:909–932.
21. **Herrero LJ, et al.** 2011. Critical role for macrophage migration inhibitory factor (MIF) in Ross River virus-induced arthritis and myositis. Proc. Natl. Acad. Sci. U. S. A. **108**:12048–12053.
22. **Hietala MA, Jonsson IM, Tarkowski A, Kleinau S, Pekna M.** 2002. Complement deficiency ameliorates collagen-induced arthritis in mice. J. Immunol. **169**:454–459.
23. **Jaffar-Bandjee MC, et al.** 2010. Emergence and clinical insights into the pathology of Chikungunya virus infection. Expert Rev. Anti Infect. Ther. **8**:987–996.
24. **Ji H, et al.** 2002. Arthritis critically dependent on innate immune system players. Immunity **16**:157–168.
25. **Kasturi SP, et al.** 2011. Programming the magnitude and persistence of antibody responses with innate immunity. Nature **470**:543–547.
26. **Kawai T, Akira S.** 2010. The role of pattern-recognition receptors in innate immunity: update on Toll-like receptors. Nat. Immunol. **11**:373–384.
27. **Kuhn RJ, Niesters HG, Hong Z, Strauss JH.** 1991. Infectious RNA transcripts from Ross River virus cDNA clones and the construction and characterization of defined chimeras with Sindbis virus. Virology **182**:430–441.
28. **Laine M, Luukkainen R, Toivanen A.** 2004. Sindbis viruses and other alphaviruses as cause of human arthritic disease. J. Intern. Med. **256**:457–471.
29. **Lidbury BA, Mahalingam S.** 2000. Specific ablation of antiviral gene expression in macrophages by antibody-dependent enhancement of Ross River virus infection. J. Virol. **74**:8376–8381.
30. **Lidbury BA, et al.** 2008. Macrophage-derived proinflammatory factors contribute to the development of arthritis and myositis after infection with an arthrogenic alphavirus. J. Infect. Dis. **197**:1585–1593.
31. **Lidbury BA, Simeonovic C, Maxwell GE, Marshall ID, Hapel AJ.** 2000. Macrophage-induced muscle pathology results in morbidity and mortality for Ross River virus-infected mice. J. Infect. Dis. **181**:27–34.
32. **Lund JM, et al.** 2004. Recognition of single-stranded RNA viruses by Toll-like receptor 7. Proc. Natl. Acad. Sci. U. S. A. **101**:5598–5603.
33. **Mandl JN, et al.** 2011. Distinctive TLR7 signaling, type I IFN production, and attenuated innate and adaptive immune responses to yellow fever virus in a primate reservoir host. J. Immunol. **186**:6406–6416.
34. Reference deleted.
35. **McKimmie CS, Fazakerley JK.** 2005. In response to pathogens, glial cells dynamically and differentially regulate Toll-like receptor gene expression. J. Neuroimmunol. **169**:116–125.
36. **McKimmie CS, Johnson N, Fooks AR, Fazakerley JK.** 2005. Viruses selectively upregulate Toll-like receptors in the central nervous system. Biochem. Biophys. Res. Commun. **336**:925–933.
37. **Morrison TE, Fraser RJ, Smith PN, Mahalingam S, Heise MT.** 2007. Complement contributes to inflammatory tissue destruction in a mouse model of Ross River virus-induced disease. J. Virol. **81**:5132–5143.
38. **Morrison TE, Simmons JD, Heise MT.** 2008. Complement receptor 3 promotes severe ross river virus-induced disease. J. Virol. **82**:11263–11272.
39. **Morrison TE, et al.** 2006. Characterization of Ross River virus tropism and virus-induced inflammation in a mouse model of viral arthritis and myositis. J. Virol. **80**:737–749.
40. **Mosmann TR, Cherwinski H, Bond MW, Giedlin MA, Coffman RL.** 2005. Two types of murine helper T cell clone. I. Definition according to profiles of lymphokine activities and secreted proteins. 1986 J. Immunol. **175**:5–14.
41. **Mosmann TR, Coffman RL.** 1989. TH1 and TH2 cells: different patterns of lymphokine secretion lead to different functional properties. Annu. Rev. Immunol. **7**:145–173.
42. **Oda K, Kitano H.** 2006. A comprehensive map of the toll-like receptor signaling network. Mol. Syst. Biol. **2**:2006.0015. doi:10.1038/msb4100057.
43. **Romagnani S.** 1995. Biology of human TH1 and TH2 cells. J. Clin. Immunol. **15**:121–129.
44. **Ryman KD, Klimstra WB.** 2008. Host responses to alphavirus infection. Immunol. Rev. **225**:27–45.
45. **Ryman KD, Klimstra WB, Nguyen KB, Biron CA, Johnston RE.** 2000. Alpha/beta interferon protects adult mice from fatal Sindbis virus infection and is an important determinant of cell and tissue tropism. J. Virol. **74**:3366–3378.
46. **Ryman KD, White LJ, Johnston RE, Klimstra WB.** 2002. Effects of PKR/RNase L-dependent and alternative antiviral pathways on alphavirus replication and pathogenesis. Viral Immunol. **15**:53–76.
47. **Shabman RS, et al.** 2007. Differential induction of type I interferon responses in myeloid dendritic cells by mosquito and mammalian-cell-derived alphaviruses. J. Virol. **81**:237–247.
48. **Shabman RS, Rogers KM, Heise MT.** 2008. Ross River virus envelope glycans contribute to type I interferon production in myeloid dendritic cells. J. Virol. **82**:12374–12383.
49. **Simone O, Tortorella C, Zaccaro B, Napoli N, Antonaci S.** 2010. Impairment of TLR7-dependent signaling in dendritic cells from chronic hepatitis C virus (HCV)-infected non-responders to interferon/ribavirin therapy. J. Clin. Immunol. **30**:556–565.
50. **Simpson DI.** 1972. Arbovirus diseases. Br. Med. Bull. **28**:10–15.
51. **Staples JE, Breiman RF, Powers AM.** 2009. Chikungunya fever: an epidemiological review of a re-emerging infectious disease. Clin. Infect. Dis. **49**:942–948.
52. **Stewart CR, et al.** 2012. Toll-like receptor 7 ligands inhibit influenza A infection in chickens. J. Interferon Cytokine Res. **32**:46–51.
53. **Takada A, Kawaoka Y.** 2003. Antibody-dependent enhancement of viral infection: molecular mechanisms and in vivo implications. Rev. Med. Virol. **13**:387–398.
54. **Takahashi K, et al.** 2010. Plasmacytoid dendritic cells sense hepatitis C virus-infected cells, produce interferon, and inhibit infection. Proc. Natl. Acad. Sci. U. S. A. **107**:7431–7436.
55. **Takeda K.** 2005. Evolution and integration of innate immune recognition systems: the Toll-like receptors. J. Endotoxin Res. **11**:51–55.
56. **Trouw LA, Daha MR.** 2011. Role of complement in innate immunity and host defense. Immunol. Lett. **138**:35–37.
57. **Tseng JC, Zheng Y, Yee H, Levy DE, Meruelo D.** 2007. Restricted tissue tropism and acquired resistance to Sindbis viral vector expression in the absence of innate and adaptive immunity. Gene Ther. **14**:1166–1174.
58. **Walport MJ.** 2001. Complement. N. Engl. J. Med. **344**:1058–1066.
59. Reference deleted.
60. **Watters TM, Kenny EF, O'Neill LA.** 2007. Structure, function and regulation of the Toll/IL-1 receptor adaptor proteins. Immunol. Cell Biol. **85**:411–419.
61. **White LJ, Wang JG, Davis NL, Johnston RE.** 2001. Role of alpha/beta interferon in Venezuelan equine encephalitis virus pathogenesis: effect of an attenuating mutation in the 5′ untranslated region. J. Virol. **75**:3706–3718.
62. **Yamamoto M, Akira S.** 2005. TIR domain-containing adaptors regulate TLR signaling pathways. Adv. Exp. Med. Biol. **560**:1–9.
63. **Yang K, et al.** 2005. Human TLR-7-, -8-, and -9-mediated induction of IFN-alpha/beta and -lambda Is IRAK-4 dependent and redundant for protective immunity to viruses. Immunity **23**:465–478.
64. **Yoneyama H, et al.** 2005. Plasmacytoid DCs help lymph node DCs to induce anti-HSV CTLs. J. Exp. Med. **202**:425–435.
65. **Zacks MA, Paessler S.** 2010. Encephalitic alphaviruses. Vet. Microbiol. **140**:281–286.
66. **Zucchini N, et al.** 2008. Overlapping functions of TLR7 and TLR9 for innate defense against a herpesvirus infection. J. Immunol. **180**:5799–5803.